A. E. Ruehli D. M. Ellis

Numerical Calculation of Magnetic Fields in the Vicinity of a Magnetic Body

Abstract: Static magnetic fields, resulting from an applied field, are calculated in the vicinity of a magnetic body. Specifically, numerical results are given for a rectangular body of constant permeability. The reduction or shielding of the magnetic fields is calculated in the neighborhood of the body. Integral equations are developed which can be solved numerically on a computer. Typical fields are described for rectangles of different thicknesses, and comparisons with known solutions are shown.

1. Introduction

With the availability of powerful present-day computers, efficient numerical methods for magnetic field calculations are being developed. One such method, based on an integral-equation approach, is discussed in this paper. The method is applicable to magnetic bodies of arbitrary shape, but special consideration is given to thin planar geometries since they are easy to fabricate by deposition techniques. In most cases the field problems involve large free space regions and are not well suited to finite difference techniques for solving Laplace's equation. A three-dimensional grid must be constructed over at least part of the free space regions for the relaxation solution, and storage requirements are exceedingly large for a solution of reasonable accuracy. This is especially true for flat geometries.

In contrast, for the integral equation techniques presented here in the numerical solution, grid points are restricted to the two-dimensional surface of the body. Thus, the difference in storage requirements between the two approaches becomes larger with a decrease in grid size. The grid or cell size can be varied rather easily in the integral equation approach, but the programming of the method is more complex than, for example, a finite difference method.

Magnetic stray fields have been calculated for elliptical bodies[1], and for bodies of a rectangular shape for low permeabilities[2]. The formulation given below is similar to a scheme used previously[3] for electrostatic

fields, and a two-dimensional vector integral equation has also been described. [4].

The methods described in this paper are generally applicable, as exemplified by their use in calculating fields for the following three basic structures: a cube, a sheet of arbitrary thickness 0.1 and, as a limiting case, an infinitely thin sheet of infinite permeability. These structures were chosen because a comparison with existing solutions[1] can thus be obtained, at least for some points in the neighborhood of the body. Also, a thin sheet represents a fairly difficult application with which to demonstrate the method.

In the following two sections, an integral equation is developed for arbitrary geometries. Numerical aspects are discussed in Section 4. Section 5 is devoted to the case of the infinitely thin sheet, and numerical results for three cases are compared with other solutions in Section 5.

2. Formulation in terms of magnetic poles

A convenient scalar formulation results if the concept of magnetic pole density is used. The definitions of Reitz and Milford[5] are adopted (rationalized MKS system) for magnetization and pole density. The fields are then related to magnetization by $\mathbf{B} = \mu_0(\mathbf{H} + \mathbf{M})$. From Maxwell's equation $\nabla \cdot \mathbf{B} = 0$ it follows that $\nabla \cdot \mathbf{H} = -\nabla \cdot \mathbf{M}$. The volume magnetic pole density is then defined by $\rho_{\rm m} = -\nabla \cdot \mathbf{M}$. The field is related to the magnetic scalar

potential U by $\mathbf{H} = -\nabla U$. An integral solution to Poisson's equation relates the pole density to the magnetic potential,

$$U(\mathbf{r}) = \frac{1}{4\pi} \int_{\mathbf{r}} \frac{\rho_{\mathbf{m}}(\mathbf{r}')}{|\mathbf{r} - \mathbf{r}'|} dv' + \frac{1}{4\pi} \int_{\mathbf{r}} \frac{\sigma_{\mathbf{m}}(\mathbf{r}')}{|\mathbf{r} - \mathbf{r}'|} da'$$
 (1)

at a point \mathbf{r} anywhere in space where s represents the surface of a magnetic body of volume v. In the second integral $\sigma_{\rm m}$ is the surface pole density. Since the magnetic material is assumed to be uniform, all induced magnetic poles reside on s, implying that $\rho_{\rm m}(\mathbf{r})=0$ in Eq. (1). The numerical solution of the integral equation in the next section gives the values of $\sigma_{\rm m}$ on s. Finally, the components of field at any point $\mathbf{r}=(x,y,z)$ are calculated by superposition as

$$H_{\gamma}(\mathbf{r}) = \frac{1}{4\pi} \int_{s} \sigma_{m}(\mathbf{r}') \frac{(\gamma - \gamma')}{|\mathbf{r} - \mathbf{r}'|^{3}} d\mathbf{a}' + H_{\gamma}^{\Lambda}, \tag{2}$$

where $\gamma = x$, y, z and H_{γ}^{A} is the projection of the applied field \mathbf{H}^{A} onto the γ -direction.

2. Integral equation for the surface pole density

An equation is derived describing the pole density at any point r on the interface between two materials of different permeability, μ^+ and μ^- . The continuity of B_n across the interface implies that

$$\mu^{+}H_{n^{+}} - \mu^{-}H_{n^{-}} = 0, \tag{3}$$

where n^+ and n^- are the normal directions into the regions of permeability μ^+ and μ^- , respectively. The surface s is assumed to be locally smooth everywhere (which is satisfied for physical systems since all corners have a small finite radius of curvature), and is divided into two surfaces, a small disk of radius ρ with center at the projection of r onto the interface as shown in Fig. 1. The remainder of the surface is called s'. The radius of the disk approaches zero in such a way that $\delta = o(\rho)$, where δ represents the normal distance between the point r and the center of the disk. Then, in the limit $\rho \to 0$, the total field on either side of the interface can be written as

$$H_{n^{\pm}}(\mathbf{r}) = \pm H_{I}(\mathbf{r}) + \frac{1}{4\pi} \int_{s'} \sigma_{\mathbf{m}}(\mathbf{r}') \ G(\mathbf{r}, \mathbf{r}') \ da' + H_{n^{+}}^{\Lambda},$$

where

$$G(\mathbf{r}, \mathbf{r}') \equiv \frac{(\mathbf{r} - \mathbf{r}')n^{+}}{|\mathbf{r} - \mathbf{r}'|^{3}}.$$
 (5)

Here, $H_{\rm p}({\bf r})=\sigma_{\rm m}({\bf r})/2$ represents the contribution of the charge layer on the small disk surface. The normal component of the applied field includes the field generated by potential currents in the system. Substituting both statements of Eq. (4) into Eq. (3), we obtain an integral equation for the pole density at r:

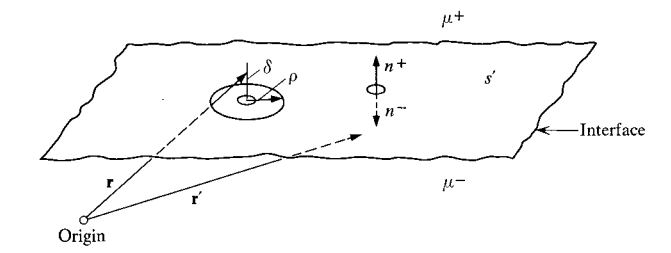


Figure 1 A section of the interface between two materials.

$$-\sigma_{\rm m}(\mathbf{r}) = \frac{R}{2\pi} \int_{a}^{b} \sigma_{\rm m}(\mathbf{r}') G(\mathbf{r}, \mathbf{r}') da' + 2RH_{n^{+}}^{A}, \qquad (6)$$

where $R = (\mu^+ - \mu^-)/(\mu^+ + \mu^-)$. Equation (6) is a Fredholm equation of the second kind and is therefore suitable for an iterative solution in its present form. Further, the convergence properties of the iterative solution are improved if an additional condition is specified:

$$\int_{a} \sigma_{\rm m}(\mathbf{r}') \ da' = 0. \tag{7}$$

3. Numerical solution for rectangular bodies

Equations (6) and (7) must be put into a discrete form suitable for a numerical solution. Approximate equations are derived specifically for the rectangular bodies under consideration. Other geometries can be considered, however, with minor modifications.

A semi-analytical approach is used to obtain the discrete surface integrals. Let the surface s be divided into a set of nonoverlapping surface cells S_j . A suitable choice consists of rectangles of side length $\Delta \gamma = l_{\gamma}/N_{\gamma}$ where N_{γ} signifies the number of divisions in the γ direction and l_{γ} is the total side length of the surface.

The surface integral in Eq. (6) can be rewritten in terms of defined intervals as

$$\int_{s} = \sum_{j=1}^{N} \int_{S_{j}},$$

where the total number of intervals is given by

$$N = 2(N_{x}N_{y} + N_{x}N_{z} + N_{y}N_{z}).$$

By the mean value theorem [6],

$$\int_{S_j} \sigma_{\mathbf{m}}(\mathbf{r}') \ G(\mathbf{r}, \mathbf{r}') \ da' = \sigma_{\mathbf{m}}(\boldsymbol{\xi}_j) \int_{S_j} G(\mathbf{r}, \mathbf{r}') \ da', \tag{8}$$

where ξ_j represents a suitable point on the surface cell S_j and $\sigma_{\rm m}(\xi_j)$ is bounded by its smallest and largest value on the interval. With the definition $\sigma_{\rm m}(\xi_j) \equiv \sigma_{\rm m_j}$ and

$$fs_{ij} = \int_{S_i} G(\mathbf{r}_i, \mathbf{r}') da', \tag{9}$$

Eq. (8) can be rewritten as

479

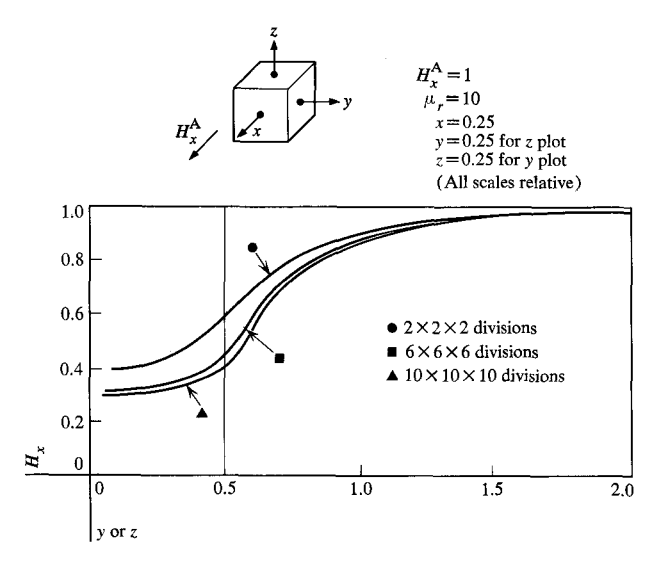


Figure 2 Variation of H_x with y or z for a cube.

$$-\sigma_{m_i} = \frac{R}{2\pi} \sum_{\substack{j=1 \ j \neq i}}^{N} \sigma_{m_j} f s_{ij} + 2R H_{n}^{\Lambda}.$$
 (10)

for $i=1, 2, \dots, N$. The integral in fs_{ij} can be evaluated analytically for the rectangular coordinate system considered. Two basic expressions result, one for n^+ normal for the cell surface S_j and one for n^+ parallel to S_j . If the field point is located on the same surface of the body as the pole density, a zero contribution results $(fs_{ij}=0)$. The matching points \mathbf{r}_i are always chosen to be at the centers of the cells.

The exact locus of ξ_j , the points where the charge densities are calculated, is in general unknown. The approximation made in the solution is then to assume that Eq. (8) is approximately satisfied if the ξ_j are located at the centers of the cells. This approximation is discussed further in the context of the numerical solutions.

Equation (10) is solved by first assuming a zero pole density on the right hand side. The left hand side leads to a new, updated value of pole density. With symmetry and a homogeneous applied field, Eq. (7) can be implemented in a particularly simple form by setting

$$\sigma_{\rm m}(\mathbf{r}) = -\sigma_{\rm m}(-\mathbf{r}). \tag{11}$$

This implies that the pole densities must be recalculated for only half the intervals, which reduces the storage requirement by a factor of two. Storage is reduced by another factor of two if one component of the applied field is zero.

Figures 2 and 3 show the inside (demagnetizing) fields and the fields in the neighborhood of a cube of normalized side length 1 with a relative permeability of 10. The x component of the magnetic field is normalized with respect to the applied field $H_x^A = 1$. The internal field is

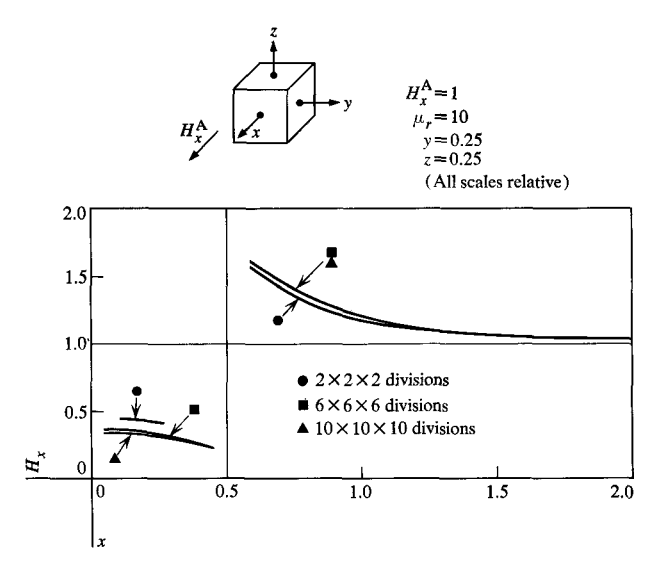


Figure 3 Variation of H_x with x for a cube.

close to that of an inscribed sphere, which is 0.25. Convergence of the solutions with respect to the number of intervals is indicated. The solutions for 36 and 100 intervals per side are almost equivalent. It is expected that a relatively small number of intervals is sufficient for $\mu_r = 10$, since the pole density is nearly constant. Equation (8) is exact for all ξ_j on the respective cells if the pole density is constant, and a small number of intervals N will lead to accurate results in this case. The computation for the cube was done on an IBM 1130 computer. Fewer than eight iterations were required in the above calculations for $\sigma_i^7 = \sigma_i^8$, $i = 1, 2, \cdots, N$, to three significant digits.

Each iteration consists of the application of Eq. (10) with a step corresponding to Eq. (7). The iteration is stopped after the *m*th step if $\sigma_i^m = \sigma_i^{m+1}$ on all cells within a specified error. The representation of the corners of the body as being curved is necessary only if the number of cells is very large, since the local field at the corners is seldom of interest. Theoretical aspects of the iterative convergence of similar schemes are discussed in [7].

4. Infinitely thin sheet of infinite permeability

For rectangular bodies with a small thickness t, the above representation becomes inexact. It is evident that the side lengths of the cells must be small compared with t. This results in an impossibly large number of cells for practical computation, and a different integral equation is therefore considered for an infinitely thin sheet of infinite permeability. The corners are not rounded in this case, and the pole density is the sum of the top and bottom pole densities. Also, the field is zero on the sheet and therefore the magnetic scalar potential is constant (U=0). The magnetic potential arising from the applied field is

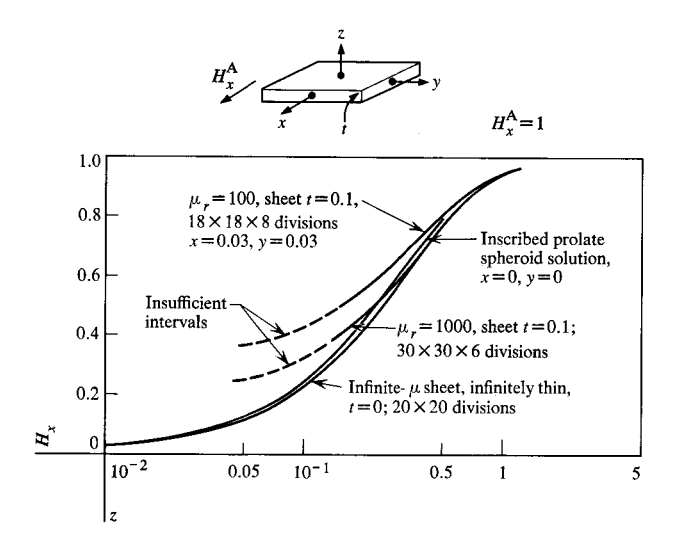


Figure 4 Variation of H_x on the top surface of a flat geometry.

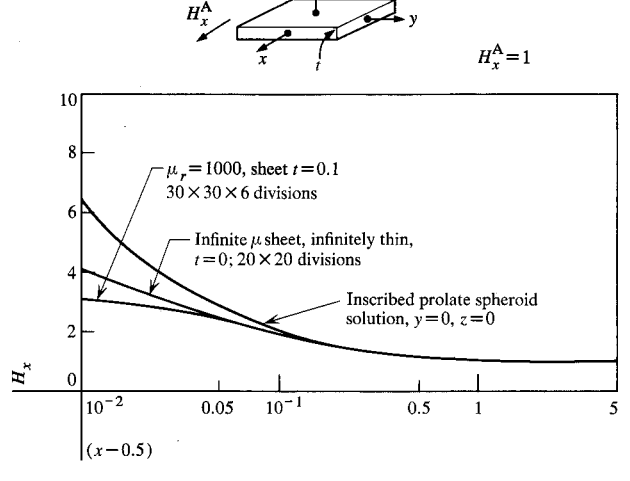


Figure 5 Variation of H_x in front of a thin sheet.

$$U_{a}(x, y) = -xH_{x} - yH_{y}.$$
 (12)

A Fredholm equation of the first kind results with Eq. (1) if the potentials are superimposed inside the sheet:

$$U_{a} + \frac{1}{4\pi} \int_{a}^{a} \frac{\sigma_{m}(\mathbf{r}') \, da'}{|\mathbf{r} - \mathbf{r}'|} = 0. \tag{13}$$

In discrete form, Eq. (13) becomes, with the same approximations as above,

$$x_{i}H_{x} + y_{i}H_{y} = \sum_{j=1}^{N} \sigma_{m_{j}}ps_{ij}; i = 1, 2, \dots, N,$$
where

$$ps_{ij} = \frac{1}{4\pi} \int_{S_i} \frac{1}{|\mathbf{r}_i - \mathbf{r}'|} da'. \tag{15}$$

Equation (14) forms a system of equations $-U_a = [ps_{ii}]\sigma_m$ with the elements of the matrix given by Eq. (15). The pole densities are immediately obtained by solving the system for the surface pole density vector $\sigma_{\rm m}$. Finally, the magnetic field H(r) is again obtained by using Eq. (2) in the same way as for the finite permeability calculations. The matrix here is of size $N_x N_y \times N_x N_y$, where N_x and N_{y} represent the number of divisions per side of the rectangle.

If cells are taken to be everywhere the same size, the matrix becomes ill-conditioned for a large number of intervals. In this case it is advisable to decrease the size for cells near the sides. The pole density vector is multiplied by the cell area with an appropriate division of the coefficients ps_{ii} by the cell area. In this way, the new solution vector is more uniform since the cell size is small where σ_{m_i} is large.

Equation (13) does not lend itself to an iterative solution as well as does Eq. (6). Of course, the system could still be solved by an iterative matrix inversion scheme. There always exists a trade-off between the computer storage requirement and computation time. For example, an iterative solution for the finite $-\mu$ case requires only N/2 words of storage if the coefficients, Eq. (9), are recomputed whenever they are needed.

5. Comparison among different solutions

Figure 4 shows the variation of the H_x component with distance from the center of the top surface of the magnetic body. The solutions given for the prolate spheroid inscribed in the square sheet are after Chang and Burns[1]. The prolate spheroid solution compares closely to the solution from the infinitely thin sheet. This is to be expected since the observation points are far from the dissimilar corner regions. Further, in Fig. 4 the solutions for the finite-thickness sheet are quite poor for distances close to the surface. This is understandable, however, if the coarse representation by the relatively large cells on the top and bottom surfaces is considered. Thus Eq. (8) is approximated rather poorly. An increase from 18 cells per side to 30 cells improves the situation considerably. By inspection of Eq. (10), it is found that the source field H_x^A enters into the equations only for the front and back poles. This implies that the pole density at the center of the sheet depends on an accurate representation of the top and bottom as well as the front and back. It can thus be concluded that the center of the sheet is the worst position for convergence with respect to the number of intervals.

The computations for the sheet with $30 \times 30 \times 6$ divisions took about 20 minutes on an IBM System/360, Model 91 computer for 16 iterations. The coefficients given by Eq. (9) were not stored between iterations.

Figure 5 shows a comparison of the three solutions for points close to the front of the sheets. Here, the solu-

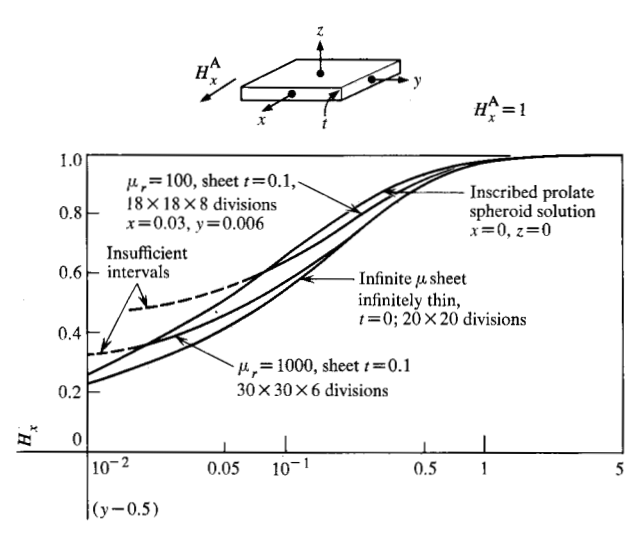
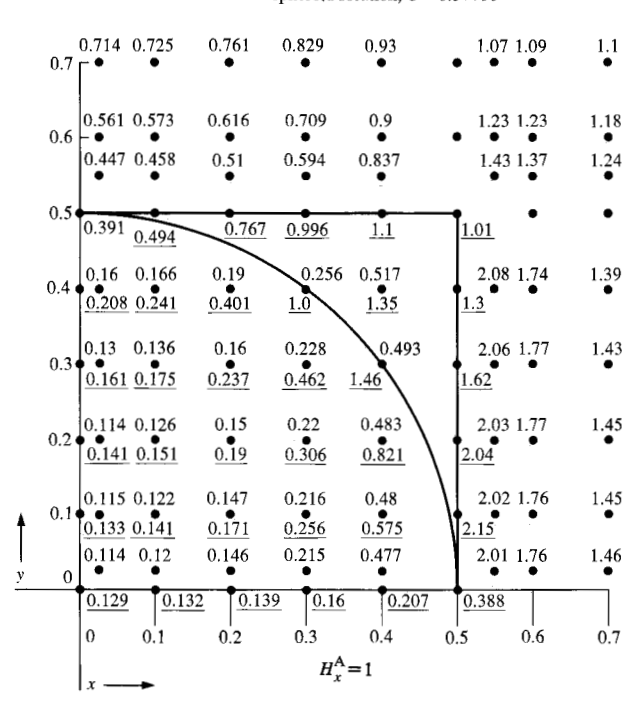


Figure 6 Variation of H_r on the side of a thin sheet.

Figure 7 Comparison of the fields above a sheet at z = 0.05.

Numbers above points: infinite- μ sheet, infinitely thin. 20 × 20 divisions

Underlined numbers below points: flat inscribed prolate spheroid solution, $C = 0.5 \times 10^{-5}$



tions for the two integral equation formulations compare rather closely, as must be expected from the above discussion. The prolate spheroid is of a considerably different shape in this region, such that the fields are overestimated. As the last location of interest, the solution near the side is shown in Fig. 6. Again, convergence with respect to the number of cells is observed for the finite- μ solution. The solutions are, however, more accurate than the solutions in Fig. 5 since coupling exists from both the top and bottom faces and also from the side faces.

Finally, the field close to the surface is shown in Fig. 7. The greatest difference in the solutions is observed near the corner region, as is expected. The fields near the surface are reduced or shielded considerably, especially near the center of the body.

Summary

Integral equation formulations have been given for the calculation of magnetic fields for magnetic bodies in external fields. The above formulation has been directed to a single body of rectangular shape. This should, however, not be interpreted to mean that the technique is restricted to a single magnetic body. The calculation of fields for multiple bodies is quite feasible if a sufficiently fast computer is available with a large storage capacity.

Special consideration has been given to the problem of flat geometries because of their practical interest, and because they represent a challenging problem. Flat geometries point out convergence problems with the size of the cells used in the numerical approximations. These problems have been discussed extensively.

Acknowledgments

The authors acknowledge helpful discussions with J. M. Daughton and W. Liniger.

References

- 1. H. Chang and J. Burns, J. Appl. Phys. 37, 3240 (1966).
- R. I. Joseph and E. Schlömann, J. Appl. Phys. 36, 1579 (1965).
- S. Rush, A. H. Turner and A. H. Cherin, J. Appl. Phys. 37, 2211 (1966).
- 4. H. K. V. Lotsch, IEEE Trans. Magnetics MAG-5, 22 (1969).
- J. R. Reitz and F. J. Milford, Foundations of Electromagnetic Theory, Addison-Wesley Publishing Co., Inc. Reading, Mass. 1960.
- T. M. Apostol, Mathematical Analysis, Addison-Wesley Publishing Co., Inc., Reading, Mass. 1957.
- 7. M. S. Lynn and W. P. Timlake, Numerische Mathematik 11, 77(1968).

Received March 8, 1971

A. E. Ruehli is located at the IBM Components Division Laboratory, Burlington (Essex Junction), Vermont 05452. D. M. Ellis is a member of the faculty in the Department of Electrical Engineering, University of Vermont, Burlington; he was a consultant to IBM during the work reported above.